

THE CONTRIBUTION OF LONG PERIOD COMETS TO THE INTERPLANETARY DUST CLOUD

M. FULLE
*Osservatorio Astronomico
Via Tiepolo 11
I-34131 Trieste
Italy*

G. CREMONESE
*Osservatorio Astronomico
Vicolo dell'Osservatorio 5
I-35122 Padova
Italy*

ABSTRACT. The numerical analysis of cometary dust tails (Fulle 1989) allows to obtain the mass loss rate, the size distribution, the ejection velocity and the orbital eccentricity of the dust grains ejected by the parent comets. All these physical quantities are necessary and sufficient to compute the comet mass contribution to the interplanetary dust cloud. We apply this method to three long period comets, namely C/Bennett 1970II, C/Bradfield 1987XXIX and C/Liller 1988V, and obtain that each long period comet injects in bound orbits at least half of the total produced mass. When we consider that a typical long period comet can produce more than 10^{14} g of dust along each perihelion passage, we obtain that the considered long period comets alone injected a input mass rate of about 10^6 g s⁻¹ of meteoroids in bound orbits during the last 20 years, a contribution which is very close to that from all short period comets.

1. Introduction

The mass of meteoroids injected by a comet into bound orbits depends on three quantities, namely: i) the time-dependent dust mass loss rate of the comet, which gives the total mass of lost dust; ii) the time-dependent size distribution of the dust grains, which gives the percentage of the total mass released in the largest grains, i.e. in meteoroids; iii) the time and size -dependent dust ejection velocity, which gives the orbital eccentricity of the dust grains, and therefore tells us if a grain is a meteoroid or not. Dust tail analysis allows a self-consistent computation of all these quantities, thus providing a method which is applied to the dust tails of long period comets Bennett 1970II, Bradfield 1987XXIX and Liller 1988V to determine their contribution to the interplanetary dust cloud.

2. The numerical model of dust tails

The dust tail model (Fulle 1989) considers $\mathcal{N}_t \times \mathcal{N}_s \times \mathcal{N}_g$ sample dust grains, where \mathcal{N}_t is the number of samples in the time interval of dust ejection, \mathcal{N}_s is the number of samples in the sizes, and \mathcal{N}_g is the number of grains of a fixed size uniformly distributed on a dust shell. It considers different ejection geometries for each of which the ejection of dust is restricted to a cone of half width w with its symmetry axis pointing toward the Sun. The position of each grain at the observation is derived from its keplerian motion, then projected into the photographic plane coordinate system (M,N), where M is the projected prolonged radius vector, so as to obtain the model distribution of the scattered light from the tail and the related kernel matrix A.

The solutions are given by minimizing the functional $[A F - I]^2 + \beta [B F]^2$, where A is the kernel matrix, I is the data vector containing the dust tail surface light intensities of the N_k images sampled in $N_N \times N_M$ points, B is a regularizing matrix weighted by β , and F is the solution vector sampled in $N_t \times N_\mu$ values, from which the dust number and mass loss rates and the time dependent and time averaged size distributions can be directly computed. The dust ejection velocity $v(t)$ is required for the computation of the matrix A , so that it must be determined by means of a trial and error procedure. The regularizing weight β tunes the constraints to our ill-posed problem: when β increases, the instability of F decreases, but so does the quality of the fit to the data. Therefore the most probable dust velocity $v(t)$ is defined as the function giving a stable and positive vector F for a regularizing weight β as small as possible.

Table 1. The mass contribution to the zodiacal cloud of long-period comets. $u = \partial \log v(t, d) / \partial \log d$, power index of the dust velocity size dependence. w , half width of the dust ejection cone: isotropic ejection (half width $w = \pi$), hemispherical ejections ($w = \pi/2$), and strongly anisotropic ejections ($w = \pi/4$). $\mathcal{N}_s, \mathcal{N}_\mu, \mathcal{N}_t$, dust samples on a dust shell, in the modified size and in time. N_t, N_μ , samples of the solution $F(t, 1-\mu)$ in time and in the modified size. N_M, N_N , samples of the N_k source images in the M and N directions. T, number of functions $v(t)$ tested to find the true solution. \mathcal{M} , total ejected dust mass (10^{14} g) for $Ap(\alpha) = 0.06$ (Hanner et al., 1990). \mathcal{M}_b , percentage of the total mass \mathcal{M} injected into bound orbits. S, symbol in Fig. 1

| u | w | \mathcal{N}_s | \mathcal{N}_μ | \mathcal{N}_t | N_t | N_μ | N_k | N_M | N_N | T | \mathcal{M} | \mathcal{M}_b | S |
|---|------|-----------------|-------------------|-----------------|-------|---------|-------|-------|-------|----|---------------|-----------------|---|
| C/1970II: 81% of the dust mass in bound orbits | | | | | | | | | | | | | |
| -1/6 | 180° | 284 | 100 | 180 | 20 | 10 | 4 | 30 | 30 | 25 | — | 80% | ○ |
| -1/6 | 90° | 143 | 100 | 180 | 20 | 10 | 4 | 30 | 30 | 18 | — | 81% | □ |
| -1/6 | 45° | 382 | 100 | 180 | 20 | 10 | 4 | 30 | 30 | 31 | — | 78% | △ |
| -1/4 | 180° | 284 | 100 | 180 | 20 | 10 | 4 | 30 | 30 | 17 | — | 80% | + |
| -1/4 | 90° | 143 | 100 | 180 | 20 | 10 | 4 | 30 | 30 | 19 | — | 86% | × |
| -1/4 | 45° | 382 | 100 | 180 | 20 | 10 | 4 | 30 | 30 | 31 | — | 81% | * |
| C/1987XXIX: 52% of the dust mass in bound orbits | | | | | | | | | | | | | |
| -1/6 | 180° | 2578 | 100 | 180 | 20 | 10 | 2 | 30 | 30 | 10 | 2.1 | 53% | ○ |
| -1/6 | 90° | 1285 | 100 | 180 | 20 | 10 | 2 | 30 | 30 | 15 | 1.8 | 53% | □ |
| -1/6 | 45° | 382 | 100 | 180 | 20 | 10 | 2 | 30 | 30 | 36 | 2.0 | 48% | △ |
| -1/4 | 180° | 2578 | 100 | 180 | 20 | 10 | 2 | 30 | 30 | 24 | 2.1 | 51% | + |
| -1/4 | 90° | 1285 | 100 | 180 | 20 | 10 | 2 | 30 | 30 | 15 | 2.7 | 67% | × |
| -1/4 | 45° | 382 | 100 | 180 | 20 | 10 | 2 | 30 | 30 | 17 | 1.6 | 38% | * |
| C/1988V: 69% of the dust mass in bound orbits | | | | | | | | | | | | | |
| -1/6 | 180° | 284 | 100 | 180 | 20 | 10 | 3 | 30 | 30 | 22 | 0.3 | 48% | |
| -1/6 | 90° | 143 | 100 | 180 | 20 | 10 | 3 | 30 | 30 | 17 | 0.4 | 70% | ○ |
| -1/6 | 45° | 382 | 100 | 180 | 20 | 10 | 3 | 30 | 30 | 15 | 0.4 | 69% | □ |
| -1/4 | 180° | 284 | 100 | 180 | 20 | 10 | 3 | 30 | 30 | 19 | 0.3 | 47% | |
| -1/4 | 90° | 143 | 100 | 180 | 20 | 10 | 3 | 30 | 30 | 20 | 0.5 | 75% | △ |
| -1/4 | 45° | 382 | 100 | 180 | 20 | 10 | 3 | 30 | 30 | 10 | 0.4 | 65% | + |
| -1/3 | 90° | 143 | 100 | 180 | 20 | 10 | 3 | 30 | 30 | 30 | 0.5 | 74% | |
| -1/3 | 45° | 382 | 100 | 180 | 20 | 10 | 3 | 30 | 30 | 31 | 0.4 | 66% | × |
| -1/2 | 45° | 382 | 100 | 180 | 20 | 10 | 3 | 30 | 30 | 24 | 0.5 | 70% | * |

The free parameters of the model are the dust bulk density and albedo (which are approximated as constant quantities in the size and phase ranges here considered), the size dependence u of the ejection velocity v , $u = \partial \log v(t, d) / \partial \log d$, where d is the dust-particle diameter, and the dust ejection anisotropy w . Since no particular value of u and w can be assumed, we show results which depend on a combination of them, so that the sensitivity of the solutions to such parameters can be directly evaluated.

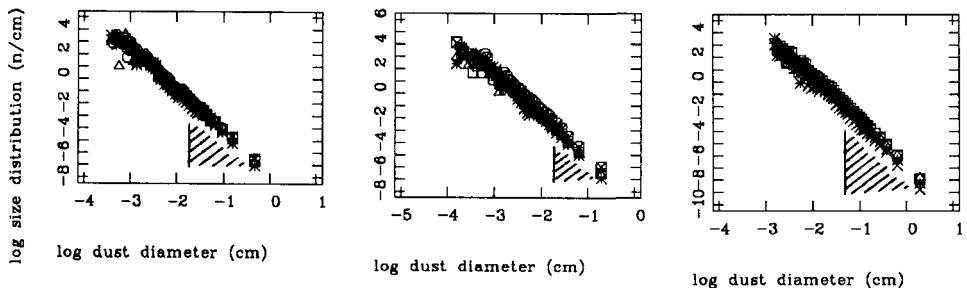
3. The meteoroid mass

The quantity F allows to directly compute the dust mass loss rate and the time-dependent size distribution, and therefore also the production rate of meteoroids, the absolute values of which depend on the dust albedo and the absolute calibration of the data, which can be affected by large uncertainties. On the contrary, the dust bulk density cannot introduce any uncertainty in the dust mass loss rate, since the relation between the dust mass and the quantity F is independent of the dust density. Moreover, if we consider the percentage of the mass production rate of meteoroids with respect to the total loss rate, we obtain a quantity which is not affected by any physical uncertainty, but only by the errors of the solution F , a good estimate of which is given by the dispersion of the solution itself due to different combinations of free parameters u and w .

We apply our model to three long period comets: four images of C/Bennett 1970II (Hogner & Richter 1980), two 20/25/50 cm Schmidt images of C/Bradfield 1987XXIX obtained by A.Cimatti, and three CCD frames of C/Liller 1988V obtained by K.Jockers and coworkers. The results are summarized in Table 1, and point out that the percentage of the meteoroid mass is independent of all on the free parameters u and w , and therefore should be affected by very low uncertainties. On the contrary, it was possible to absolutely calibrate only the Bradfield and Liller images, assuming a dust albedo for the phase function of 0.06 (Hanner et al. 1990). Since such value is an upper limit for the dust albedo of this comet, and since the model can consider only finite time and size intervals, the absolute values of the produced dust mass should be considered as lower limits only.

Our results point out the high percentage of meteoroids produced by all the long period comets here considered. This fact is mainly due to the high power index of the size distributions of such comets, which are shown in Fig.1. All the power indexes are significantly higher than -4 , and this fact implies that most of the mass is released in large grains, i.e. in meteoroids, the size range of which is also shown in the same figure.

Fig.1 Time averaged size distributions of C/1970II (left, power index -3.3 ± 0.1), C/1987XXIX (center, power index -3.2 ± 0.2) and C/1988V (right, power index -3.5 ± 0.1). The dust bulk density is assumed of 1 g cm^{-3} (the diameter values d depend inversely on the assumed dust bulk density). The symbols are related to Table 1. The shaded areas show the size range of the meteoroids in bound orbits.



4. Discussion

When we remember that C/Bennett was by far brighter than comet Bradfield, we can conclude that in the last 20 years at least 3 long period comets contributed to the zodiacal dust cloud, with an averaged meteoroid loss of at least 10^{14} g for each comet. If we admit that such a sample has statistical significance (such a very poor statistic obviously needs further samples), we obtain from the long period comet family $\approx 10^6$ g s⁻¹ of meteoroids in orbits bound in the Solar System, a value 30 times larger than the statistical estimate by Mukai (1990). Such disagreement points out that each long period comet has to be deeply analysed to deduce its effective production of meteoroids injected into bound orbits.

Our model applied to Schmidt plates (from Sekanina & Schuster 1978a,b) of short period comets Encke and D'Arrest has shown that each short period comet injects in bound orbits $\approx 5 \cdot 10^4$ g s⁻¹ of meteoroids (Fulle 1990), an estimate very close to the results of the analysis of IRAS dust trails (Sykes 1990). Therefore the contribution of meteoroid mass from long period comets is close (probably a bit lower) to that from ≈ 100 short period comets, in agreement with the significant percentage of observed meteoric orbits which can be explained only in terms of a long period cometary source (Olsson-Steel 1990).

The long period cometary source would supply an isotropic dust cloud, because the Poynting-Robertson drag does not change the orbital inclinations. However the meteoroids from short period comets cover all the sizes observed in the related dust tails ($d > 20$ μ m for a dust bulk density of 1 g cm⁻³, here the sizes depend inversely on the adopted dust density), whereas only the largest grains from long period comets become meteoroids ($d > 200$ μ m). Therefore the optical scattering from short period meteoroids is much larger than from long period ones (a factor 10 in the case of a size distribution power index of -4), so that also in the limit case of the same input mass rate from the two cometary sources, we would obtain a strong optical concentration of zodiacal dust close to the ecliptical plane.

The different distribution of orbital inclinations of the two cometary sources implies a strong correlation between ecliptical latitude and meteoroid size distribution. Very far from the ecliptic we should find no cometary meteoroids in bound orbits for $d < 0.2$ mm, but a significant mass for $d > 0.2$ mm, a bit lower than close to the ecliptical plane.

5. References

- Fulle, M. (1989) Evaluation of cometary dust parameters from numerical simulations: comparison with analytical approach and role of anisotropic emissions. *Astron. Astrophys.* **217**, 283 - 297
- Fulle, M. (1990) Meteoroids from short period comets. *Astron. Astrophys.* **230**, 220 - 226
- Hanner, M.S., Newburn, R.L., Gehrz, R.D., Harrison, T., Ney, E.P., Hayward, T.L. (1990) The infrared spectrum of Comet Bradfield (1987s) and the silicate emission feature. *Astrophys.J.* **348**, 312 - 321
- Hogner, W., Richter, N. (1980) *Isophotometric Atlas of Comets*, Par. II, Springer-Verlag
- Mukai, T. (1988) Dust from the comets. *Highlights of Astronomy* **8**, 305 - 312
- Olsson-Steel, D. (1990) The orbital distribution and origin of meteoroids. *Origin and evolution of interplanetary dust (126th IAU Colloquium)* Kluwer Academic Publisher
- Sekanina, Z., Schuster, H.E. (1978a) Meteoroids from Periodic Comet D'Arrest. *Astron. Astrophys.* **65**, 29 - 35
- Sekanina, Z., Schuster, H.E. (1978b) Dust from Periodic Comet Encke: Large Grains in Short Supply. *Astron. Astrophys.* **68**, 429 - 435
- Sykes, M. (1990) Cometary and asteroidal sources of interplanetary dust. *Origin and evolution of interplanetary dust (126th IAU Colloquium)* Kluwer Academic Publisher